



ORIGINAL RESEARCH ARTICLE

OPTIMIZATION OF PROCESS PARAMETERS ON FATIGUE AND COMPRESSIVE STRENGTH OF AL7075/COCONUT SHELL ASH COMPOSITE

A. V. Gambo^{1*}, C. O. Njoku², Y. Bello³

¹Department of Mechanical Engineering, Ahmadu Bello University, Zaria

²Department of Mechanical Engineering, Air Force Institute of Technology, Kaduna

³Department of Mechatronics Engineering, Air Force Institute of Technology, Kaduna

*Corresponding authors' email: gambo.anthony@yahoo.com

ARTICLE INFORMATION

Received: 29th August 2025
Revised: 12th November 2025
Accepted: 13th November 2025

Keywords:

Composite
Coconut shell ash
Grey relational analysis
ANOVA

ABSTRACT

The study investigates the effect of coconut shell ash particulate (CSAp) on the fatigue and compressive strength of Aluminium (Al) 7075 metal matrix composite; and optimized by Taguchi Grey Relational Analysis (GRA). The composites were prepared by conventional double stir casting method with varying coconut shell ash content (5wt%, 10wt%, 15wt% and 20wt%). Five factors, four levels Taguchi experimental design were used to optimize the number of experiments. The factors considered were reinforcement fraction, processing temperature, stirring speed, stirring time and particle size of Al/CSAp reinforcement in the matrix. Taguchi L_{16} orthogonal array was employed in fabricating different samples of the composite. The significant effect of the experimental design parameters on the responses was investigated using analysis of Variance (ANOVA). The results for the fatigue strength of the Aluminium/CSAp composite showed that processing temperature with a contribution of 57.55% has the highest influence on the fatigue; followed by reinforcement fraction with 11.49%, particle size with 14.25%, stirring speed with 8.93%, and stirring time with 1.11% in addition, the ANOVA for compressive strength of the composite showed that stirring speed with a contribution of 70.38% has the highest influence on the compressive strength; followed by particle size, with 24.22%, processing temperature, with 0.55%, reinforcement fraction, with 0.11%, and stirring time, with 0.06%. The optimal combination for the Taguchi grey relational analysis was coconut shell ash particles at 10wt%, stirring speed at 600rpm, processing temperature at 850°C, stirring time at 120secs, and particle size at 25 μ m. Stirring speed and processing temperature were considered significant contributors to the change in grey relational grade (GRG) of the composite. Confirmatory experiments carried out using the optimal parameters (CSAp₂SS₄PT₃ST₂PS₁) showed an improvement in the fatigue and compressive strength of the optimized composite of 36.4% and 30.7% over the initial settings.

© 2025 Faculty of Engineering, University of Maiduguri, Nigeria. All rights reserved.

1.0 Introduction

The search for low-cost alternatives in Aluminium metal matrix composites (AMC) production has led to a number of efforts tailored at utilizing industrial and natural fibres as reinforcing materials (Baradeswara et al., 2012). AMCs are the most commonly utilized metal matrix composites due to several reasons, including ease of processing, lower cost compared to other metal matrices and favorable physical and mechanical properties. Due to these outstanding properties, a great number of research works have been explored to understanding the influence of reinforcement parameters on the properties of AMCs (Alaneme and Adewuyi, 2013). The abundance of natural fibres has tempted researchers to try locally available fibres and to some extent they satisfy the required specifications as good reinforcement for aluminium metal matrix composites. Natural

fibres such as jute, coir, cotton, sisal and banana have attracted the attention of scientists for application in consumer goods, low-cost housing and other civil structures. It has been found that these natural fiber composites possess better electrical resistance, good thermal and acoustic insulating properties and higher resistance to fracture (Gambo, 2017). Natural fibres have advantages compared to synthetic ones such as low weight, low density, low cost, acceptable specific properties and they are recyclable and biodegradable (Gambo, 2017). They are also renewable and have relatively high strength and stiffness and cause no skin irritations (Alaneme and Adewuyi, 2013). Amongst the numerous reinforcement materials, coconut shell particles are an emerging reinforcement because of its low cost, and availability in large quantity. Madakson *et al.*, (2012) investigated the characteristics of coconut shell ash. The microscopic analysis revealed that element like SiO_2 , Al_2O_3 , MgO and Fe_2O_3 as major constituents and hard in nature leads to its utilization in automobile applications. As coconut shell ash has high thermal stability with low density, can be used in producing composite products with good thermal resistance. Apasi *et al.*, (2016) studied the microstructure and mechanical properties of aluminum alloy (Al-Si-Fe) reinforced with coconut shell-ash particulate. In their investigation, the aluminium (Al-Si-Fe) alloy composite was produced by double-stir casting process at a speed of 700 rpm for 10 and 5 minutes at first and second stirring respectively. The samples produced from addition of 0-15wt% coconut shell ash particles (CSAp) were prepared and subjected to microstructural and mechanical properties testing. The results of the microstructural analysis of the composite revealed a fairly uniform distribution of the coconut shell-ash particles in the matrix with increase in volume fraction of CSAp. The mechanical property test results revealed that, hardness of the developed composite increased with increasing percentage weight of CSAp. Also, the tensile and yield strength at 0.2% offset values of Al-Si-Fe/CSAp composite increased with percentage increase in CSAp up to 9% addition above which a little decrease in both tensile and yield strength was observed. Varalakshmi *et al.*, (2019) analyzed the dry sliding wear behaviour of Al6061- Coconut shell ash metal matrix composites using Stir casting. They found out that with more percentage of CSA addition there was an improvement in specific strength of the composite. The Taguchi analysis revealed improved specific strength as well as wear resistance. EDS analyses showed the presence of oxide phases in the castings. Franklin *et al.*, 2022, focused on the determination of the mechanical properties of coconut shell ash reinforced aluminum A356 composite. Double stir casting method was adopted in the development of the composite with a temperature of 750°C and a stirring speed of 600 rpm. The composite was produced from the addition of 0-30 wt% coconut shell ash particles to the Aluminum. The study revealed that the addition of coconut shell ash to aluminum increased the hardness and tensile strength of the composite. Also, the density and impact energy of the specimen decreased with the increase of reinforcing particles. The study implied that aluminum composite with high strength low weight recommended that Aluminum with light weight, higher tensile and hardness can be achieved by adding coconut shell ash to the parent material. With reference to available literature, it is apparent that many studies have been carried out on the development of Al/Coconut shell ash composite, but limited study is available on the optimization of the fatigue and compressive strength properties of 7075 Al/Coconut shell ash composite with selected process parameters by employing Grey Relational Analysis.

2. Materials and Methods

2.1 Materials

Aluminium alloy (7075) with elemental composition shown in Table 1; procured from NOCACO, Kaduna, Nigeria, was used as the base material for this research. Coconut shell obtained from a local market in Kafanchan, Kaduna State, was utilized as reinforcing particulate. Analytical grade (99.5%) Magnesium Turnings was used for enhancing wettability between the Al alloy and the reinforcement.

Table 1: Composition of 7075 Aluminum Alloy

Element	Al	Si	Fe	Cu	Mn	Mg	Others
Wt%	94.3	0.8	0.5	1.7	0.2	1.9	0.6

Note: Adapted from Kabelmetal Nigeria Plc technical brochure (2022)

2.2 Method

2.2.1 Production of coconut shell ash particulate

The procured coconut shells were sun dried for one month, after which they were crushed into smaller pieces, this was carried out according to the methods used by Apasi (2014). The crushed coconut shell was grinded, using a disc grinder to obtain the powder of varying mesh sizes of 25 μm , 50 μm , 75 μm and 90 μm . The Corresponding author's email address: gambo.anthony@yahoo.com

powder was packed in a graphite crucible, and fired in an electric muffle furnace at a temperature of 900°C for 1 hour to form the coconut shell ash (CSAp) as shown in Plate 1.

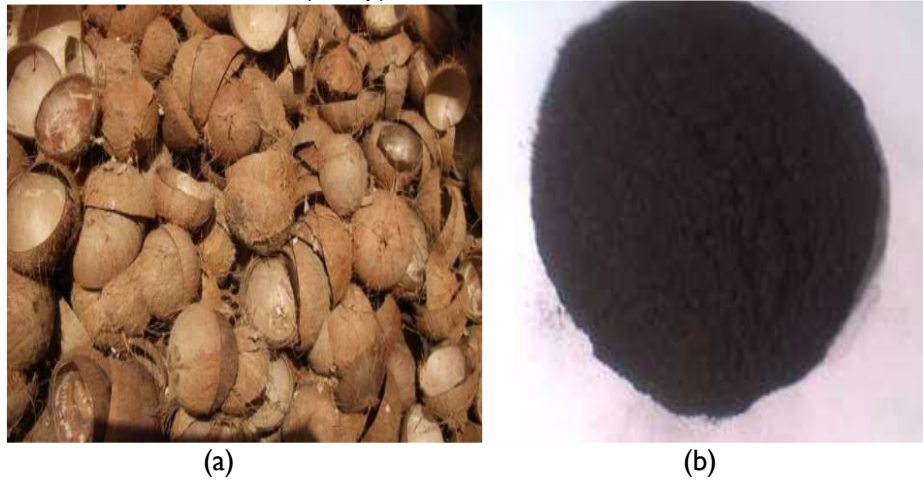


Plate 1: (a) Coconut shell (b) Coconut shell ash

2.2.2 Design of experiment (DOE)

The experiments were designed based on the Taguchi L_{16} Orthogonal Array (OA). The experimental runs were designed using five factors and four levels as indicated in Table 2. The stir casting process factors; Reinforcement fraction (wt%), Stirring speed (rpm), Processing temperature ($^{\circ}\text{C}$), Stirring time (secs), and Size of reinforcement (μm) with their levels, and feasible limit of control were selected as conducted by Adebisi and Ndaliman (2015); Kumar *et al.*, (2017); Ibrahim (2023). The outcome of the analysis was carried out using Minitab software which gives L_{16} orthogonal array.

Table 2: Processing Factors and their Levels in Taguchi Experimental Design Plan

Factors	Level 1	Level 2	Level 3	Level 4
Reinforcement fraction (wt %)	5	10	15	20
Stirring speed (rpm)	300	400	500	600
Processing temperature ($^{\circ}\text{C}$)	750	800	850	900
Stirring time (secs)	90	120	150	180
Particle size (μm)	25	50	75	90

2.2.3 Sample preparation

Production of the Al7075/CSAp composite was carried out by the double stir-casting method according to the methods used by Pulkit (2012); Aigbodion *et al.*, 2014; Adebisi and Ndaliman (2015) in a coal fired furnace, depicted in Plate 2a. Initially, the aluminium alloy was charged into a graphite crucible in the furnace, the aluminium was heated to about 750 $^{\circ}\text{C}$ till the entire alloy in the crucible is melted. The reinforcement particles (CSAp) was preheated to 800 $^{\circ}\text{C}$ for 1 hour to make its surface oxidized. The furnace temperature was cooled down just below the liquidus temperature of Aluminium, to keep the slurry in a semi-solid state. Stirring was carried out at varying times, and at a stirring rate as per the experimental design. At this stage, the preheated CSAp was added manually into the vortex. The slurry was again heated to a fully liquid state and mixed thoroughly, after the molten metal have completely melted, 0.05wt% degassing tablets (hexachloroethane) was added to reduce porosity. Simultaneously, 1wt% magnesium was added to the melt to enhance the wettability between coconut shell ash particles and the alloyed melt. After the stirring process, the mixture was poured into a sand mold and allowed to solidify to form the Al/CSAp composite as depicted in Plate 2b.

2.2.4 Fatigue test

Fatigue is the degradation of mechanical properties leading to the failure of a material or a component under cyclic loading (ASTM E606-92). The Experiments were carried out under axial constant amplitude to determine the S-N curve. The fatigue test was conducted using an Instron E3000 fatigue testing machine, of 3KN load capacity. The jaws of the machine are driven by an electric-magnetic engine, which pushes the centre of the specimen up and down with regards to the vertical axis of the load. The waveform of the fatigue test was sinusoidal, and all fatigue tests was performed under a constant frequency of 4Hz, and constant load amplitude, with a stress ratio of (R= -1 fully reversed). The load applied during the fatigue test was less than the yield stress by a factor of 0.9, to reach the failure points for high cycle fatigue; then the load was reduced

by a factor of 0.1 for each test. Test samples depicted in Plate 3, were prepared following ASTM E606-92, and to obtain the S-N curve for Fatigue testing, 8 points were required, as recommended by ASTM E606-92. The S-N curve is the plot of stress versus the number of cycles needed to fail.

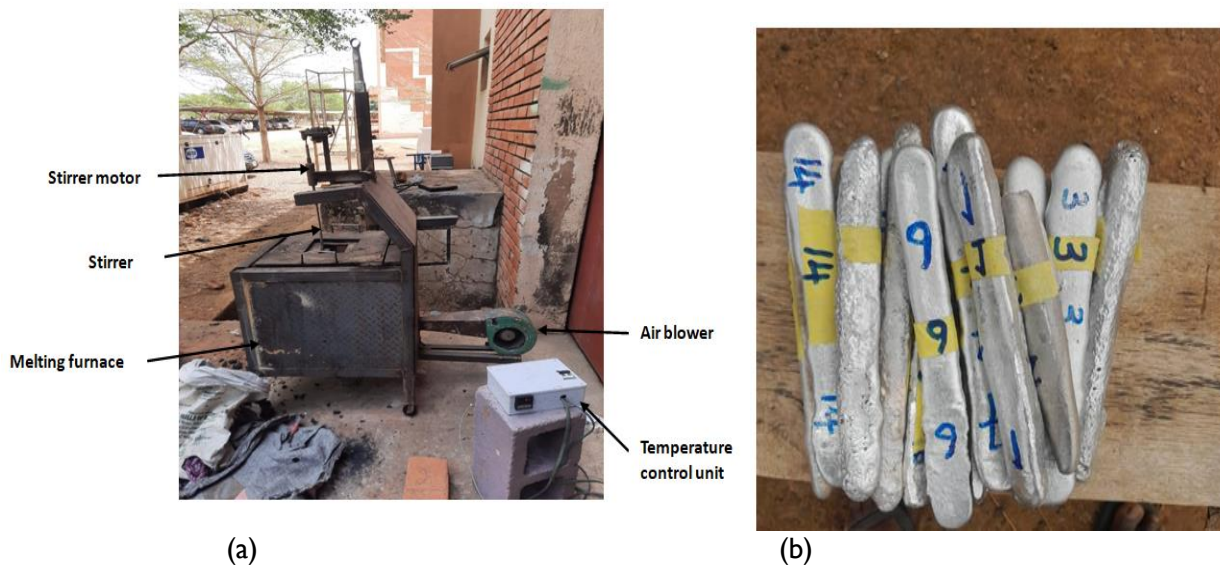


Plate 2: (a) Coal fired stir casting furnace (b) Fabricated Al7075/CSAp composite



Plate 3: Fatigue test samples

2.2.5 Compressive strength test

Compressive strength test was conducted in accordance with ASTM E09-89a (2000) on the specimens produced, which had dimension of 25mm in diameter and 75mm in length. The test was carried out on a universal testing machine. In carrying out the experiment, test samples were placed between the surfaces of the compression tool and were aligned with the centre line of the plunger. The samples were subjected to quasi static compression loading. For each specimen, the compression test was performed three times for the purpose of repeatability and reliability, and the average results were taken.

2.2.6 Taguchi optimization and GRA techniques

The Grey Relational Analysis (GRA) was employed to handle the ambiguity of many variables. The objective function employed in the optimization of the performance characteristics were based on “the higher the better”. The S/N ratio is used for maximizing the performance while minimizing the variance. In respect to these objectives, Equation 1 was used to determine the S/N (Ibrahim et al., 2023a; Ibrahim et al., 2023b):

$$\left(\frac{S}{N}\right)_{HTB} = -10 \log_{10} \left(\frac{1}{n} \sum_{i=1}^n \frac{1}{y_i^2} \right) \quad 1$$

The grey relational analysis was employed for the multi-response optimization, and the Taguchi optimization technique was applied to optimize the grey relational grade. In applying the grey relational analysis, the measured effects (Fatigue and Compressive strength) were normalized i.e. brought to a comparable value which is between zero and one. The normalization was carried out by applying Equation 2 (Raut et al., 2016; Ibrahim, 2023).

$$x_i^*(k) = \frac{x_i(k) - \min x_i(k)}{\max x_i(k) - \min x_i(k)} \quad 2$$

where; $x_i^*(k)$ is the sequence after the data processing i.e. for the i^{th} experiment and the k^{th} response and $x_i(k)$ is the comparability sequence. The reference sequence in this study was taken as 1 for all the responses. That is $x_0^*(k) = 1$.

The deviation sequence $\Delta_{0i}(k)$ which is the deviation of the reference sequence $x_0^*(k)$ and the comparability sequence $x_i^*(k)$ was calculated using Equation 3 (Raut et al., 2016; Ibrahim, 2023).

$$\Delta_{0i}(k) = |x_0^*(k) - x_i^*(k)| \quad 3$$

Where; $\Delta_{0i}(k) = 1$ -normalised value of the response

Then the grey relational coefficient (GRC) was calculated with the pre-processed sequence. The GRC is an expression of the relationship between the actual normalized results and the ideal. The GRC $\xi(k)$ is expressed in Equation 4 (Kundu and Singh, 2016).

$$\xi(k) = \frac{\Delta_{min} + \zeta \Delta_{max}}{\Delta_{0i}(k) + \zeta \Delta_{max}} \quad 4$$

where $\Delta_{0i}(k)$ is the deviation sequence of the reference sequence, $x_0^*(k)$, and the comparability sequence is $x_i^*(k)$. While ζ is the distinguishing or identification coefficient which defines the level of importance or influence of the measured response to the final objective. Since the responses were given equal preference, they were assigned an identification coefficient, $\zeta = 0.5$.

Upon the calculation of the grey relational coefficient for each experiment ($i=1, 2, 3... 9$) and each response 'k' (fatigue and compressive strength), the grey relational grade γ_i was calculated; which is the average of the coefficients from each factor and for each run. The grey relational grade γ_i as expressed by Sylajakumari et al., (2018) is shown in Equation 5.

$$\gamma_i = \frac{1}{n} \sum_k \xi_i(k) \quad 5$$

where γ_i = Grey relational grade for i^{th} experiment, n = number of performance characteristics, which is the number of responses, k .

Then the result was ranked and a response table was created using equations as detailed in the Taguchi approach. The optimum grey relational grade was predicted using Equation 6 (Raut et al., 2016; Ibrahim, 2023).

$$T_{opt} = T_m + \sum_{k=1}^{k_n} [(T_{ik})_{max} - T_m] \quad 6$$

Where T_m is the overall mean of GRG; T_{ijmax} is the mean GRG of optimum level i of factor k and k_n is the number of main design factors that affect the response (GRG). T_{ijmax} was obtained from the response table of mean or S/N ratio in which for each parameter on the table, the highest value among the levels is the T_{ijmax} .

3. Results and Discussion

3.2 Effect of the Control Factors on Fatigue

The experimental data of fatigue from the analysis were converted into S/N ratios using Equation 1. The predominant control factors were identified from the delta value in the response table for signal-noise ratio as shown in Table 3. The delta values were computed based on the difference between the highest and the lowest average value of each factor. Ranks were then assigned according to the delta value. The highest value

of delta was assigned the first rank and represents the predominant factor affecting fatigue. According to Table 3, the processing temperature (PT) emerged as the most significant factor; followed by particle size (PS) as the second most impactful factor, then reinforcement fraction (CSAp), succeeded by the stirring speed (SS), and finally, the stirring time (ST).

Table 3: Response for S/N of Fatigue Higher-the-Better

Level	CSAp	SS	PT	ST	PS
	(wt %)	(rpm)	(°C)	(Secs)	(µm)
1	1.554	1.378	1.171	1.476	1.792*
2	1.337	1.557	1.446	1.607*	1.565
3	1.613	1.608	1.685	1.597	1.502
4	1.734*	1.695*	1.937*	1.559	1.379
Delta	0.398	0.316	0.767	0.130	0.414
Rank	3	4	1	5	2
Optimum CSAp ₄ SS ₄ PT ₄ ST ₂ PS ₁					

*Optimum factor levels

The effect of various process parameters on the fatigue of the composite were obtained from the graphs drawn by taking the effect of each parameter at each level on the response. The main effects plot for signal-noise was generated as shown in Figure 1. The trend of the plot indicates that Fatigue strength of the composite is adversely influenced by the variation in processing temperature. The fatigue cycles to failure increases as the processing temperature increased. The increase could be attributed to more refined micro structural grains and a close up of the grain boundary due to increased melt viscosity at a higher temperature. This trend is consistent with a study conducted by Yekini *et al.*, (2020). The association between particle size and the S/N ratio in Figure 1 shows a decreasing trend from 1.792×10^6 cycles to 1.565×10^6 cycles. The plot of reinforcement fraction shows a decrease upon an increase in the volume fraction of coconut shell ash particles from 5 to 10 wt%; beyond this point, the fatigue cycles to failure increased with a further increase of the CSAp particles; then decreased. The relationship between the stirring speed and the S/N ratio depicts a decrease in the fatigue strength. Lastly, the trend between the stirring time and the fatigue cycle to failure indicates a positive relationship. In analyzing S/N ratio, irrespective of the quality characteristics, a higher S/N ratio conforms to better values of experimental results in this scenario higher fatigue strength. This is in agreement with the work of Yekini *et al.*, (2020). The response table and the main effects plot for S/N ratios put forward that CSAp₄SS₄PT₄ST₂PS₁ are the optimum factor levels in order to achieve high S/N ratios and higher values of Fatigue.

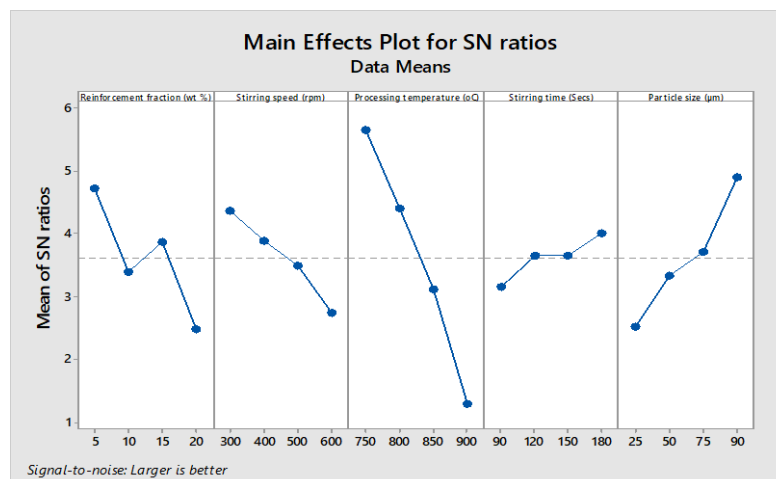


Figure 1: Main effects plot for signal-noise for fatigue

ANOVA was used to investigate whether the experimental design parameters have significant effect on the response. The analysis generated an ANOVA table which shows the level of significance of each processing parameter. The analysis was also used to develop the predictive mathematical model for the fatigue as a function of the stir casting process parameters.

Table 4 shows the ANOVA results obtained for the fatigue of the Aluminium/CSAp composite. it can be observed that processing temperature with a contribution of 57.55% has the highest influence on the fatigue;

followed by reinforcement fraction with 11.49%, particle size with 14.25%, stirring speed with 8.93%, and stirring time with 1.11%. At 95% confidence level, factors having *p*-value less than 0.05 are considered significant; our findings align with those of Sylajakumari, et al., (2018). Since the *p*-values of reinforcement fraction, stirring speed, processing temperature, and particle size are less than 0.05, they are considered significant contributors to the change in fatigue life of the composite. Conversely, stirring time is said to be an insignificant term, because its *p*-value is above 0.05.

Table 4: Analysis of Variance for Fatigue of Al/CSAp Composite

Source	DF	Seq SS	Contribution	Adj SS	Adj MS	F-Value	P-Value
Regression	5	2.09036	93.32%	2.09036	0.41807	27.96	0.000
CSAp	1	0.25730	11.49%	0.25730	0.25730	17.21	0.002
SS	1	0.20010	8.93%	0.20010	0.20010	13.38	0.004
PT	1	1.28905	57.55%	1.28905	1.28905	86.22	0.000
ST	1	0.02482	1.11%	0.02482	0.02482	1.66	0.227
PS	1	0.31909	14.25%	0.31909	0.31909	21.34	0.001
Error	10	0.14951	6.68%	0.14951	0.1495		

The developed regression model for fatigue has high coefficient of determination (R^2), R^2_{adj} and R^2_{pred} values of 93.32%, 89.99%, 84.70%, respectively. This indicates the goodness of fit between fatigue and the stir casting process parameters. Our results support previous research by Dan-Asabe (2018); Sivaiah and Chakradhar (2019) who stated that an R-sq value greater than 75% is deemed adequate.

3.3 Effect of the Control Factors on Compressive Strength (CS)

The dominant control factors were identified from the delta statistics in the response table for signal-noise ratio in Table 5. The delta statistics were computed based on the difference between the highest and the lowest average value of each factor. Ranks were then assigned according to the delta value. The highest value of delta was assigned the first rank and represents the predominant factor affecting CS. According to the table, the stirring speed (SS) emerged as the most significant factor, followed by particle size (PS), then stirring time (ST), succeeded by processing temperature (PT), and finally the reinforcement fraction (CSAp).

Table 5: Response for S/N of Compressive Strength Higher-the-Better

Level	CSAp	SS	PT	ST	PS
	(wt %)	(rpm)	(oC)	(Secs)	(μm)
1	55.04	53.85	54.92	55.29	55.89*
2	55.19	54.73	55.34*	54.87	55.54
3	55.25	55.78	55.29	55.32*	54.94
4	55.27*	56.40*	55.20	55.28	54.38
Delta	0.23	2.55	0.43	0.45	1.51
Rank	5	1	4	3	2
Optimum CSAp ₄ SS ₄ PT ₂ ST ₃ PS ₁					

*Optimum factor level

Figure 2 depicts the main effects plot for signal-noise ratios for compressive strength of the composite. The relationship between reinforcement fraction, stirring speed, particle size and the S/N ratio of the compressive strength in Figure 2 shows increasing trends. The plot of processing temperature shows that the S/N ratio value of compressive strength increased upon an increase in temperature up to the maximum of 55.34 (level 2). With further increase in temperature, the compressive strength decreased. The increase could result from the decrease in the melt viscosity. The decrease in viscosity decreases the contact angle between the melt aluminium alloy and the reinforcement, thereby enhancing the distribution and wettability of the reinforcement in the matrix. Conversely, the decrease in compressive strength could be attributed to the absorption of gases into the melt and formation of intermetallic phases at high temperature in the fabricated composite. This study is consistent with Ibrahim et al., (2023b); in which they revealed that by increasing the stirring temperature above the optimum, a less homogeneous distribution of the particles and formation of undesirable phases could be obtained in the matrix alloy, which can have an adverse effect on the composite. The compressive strength of the composite decreases as the stirring time increases, upon reaching the minimum value of 54.87 it reverses. The decrease can be attributed to non uniformity in the distribution of the reinforcement in the aluminium matrix composite due to limited stirring time. The response table and the main effects plot for S/N

ratios indicates that $CSA_{p4}SS_{4}PT_{2}ST_{3}PS_{1}$ are the desired factor levels in order to achieve high S/N ratios and higher values of compressive strength.

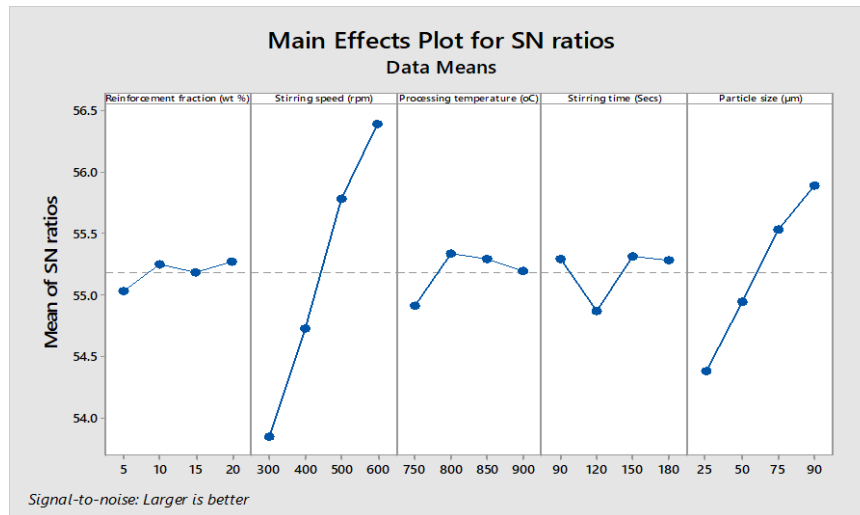


Figure 2: Main effects plot for signal-noise for compressive strength

Table 6 shows the ANOVA results obtained for the compressive strength of the Aluminium/CSAp composite. The table indicates that the stirring speed, contributing 70.38%, has the greatest effect on compressive strength; followed by particle size, with 24.22%, processing temperature, with 0.55%, reinforcement fraction, with 0.11%, and stirring time, with 0.06%. At 95% confidence level, factors having p -value less than 0.05 are considered significant; similar findings were reported by Sylajakumari, *et al.*, (2018). Since the p -values of stirring speed and particle size are less than 0.05, they are considered significant contributors to the change in compressive strength of the composite. Conversely, reinforcement fraction, processing temperature, and stirring time are said to be insignificant terms, because their p values are above 0.05.

Table 6: Analysis of Variance for Compressive Strength of Al/CSAp Composite

Source	DF	Seq SS	Contribution	Adj SS	Adj MS	F-Value	P-Value
Regression	5	88979.0		88979.0	17795.8	40.81	0.000
CSAp	1	107.1	0.11%	107.1	107.1	0.25	0.631
SS	1	65690.4	70.38%	65690.4	65690.4	150.64	0.000
PT	1	517.5	0.55%	517.5	517.5	1.19	0.302
ST	1	53.7	0.06%	53.7	53.7	0.12	0.733
PS	1	22610.2	24.22%	22610.2	22610.2	51.85	0.000
Error	10	4360.7	4.67%	4360.7	436.1		
Total	15	93339.7	100.00%				

The developed regression model for compressive strength has high coefficient of determination (R^2), R^2_{adj} and R^2_{pred} values of 95.33%, 92.99%, 88.30%, respectively. This indicates the goodness of fit between compressive strength and the stir casting process parameters.

3.4 Multiple Responses Optimization Using GRA

Preprocessed data were computed from the experimental data of the responses obtained in the Taguchi experimental design for Fatigue and Compressive strength as shown in Table 7. The normalization of data was done using Equation 2. While the deviation sequences were generated using Equation 3. Once, the deviation sequences were obtained, the grey relational coefficient (GRC) for each value of the responses was computed using Equation 4. Lastly, the mean of the GRCs was calculated to determine the GRG using Equation 5. From the analysis of the results in Table 7, experiment No.8 has the highest value of the GRG, which corresponds to better performance

Table 7:GRC and Rank of GRG with S/N Ratios

Run S/N	Factors					Responses		GRG		Ranks
	KCp (wt%)	SS (rpm)	PT (°C)	ST (Secs)	PS (µm)	Fatigue	Compressive strength	Mean	S/N Ratio (dB)	
1	5	300	750	90	25	0.6925	0.4065	0.5495	-5.20065	5
2	5	400	800	120	50	0.6258	0.452	0.5389	-5.36984	7
3	5	500	850	150	75	0.4766	0.4931	0.4849	-6.28696	10
4	5	600	900	180	90	0.5624	0.4314	0.4969	-6.07462	9
5	10	300	800	150	90	0.3599	0.7452	0.5526	-5.15178	4
6	10	400	750	180	75	0.3855	0.7331	0.5593	-5.04710	3
7	10	500	900	90	50	0.4793	0.3333	0.4063	-7.82306	14
8	10	600	850	120	25	1.0000	0.3509	0.6753	-3.41007	1
9	15	300	850	180	50	0.4744	0.4936	0.484	-6.30309	11
10	15	400	900	150	25	0.732	0.3463	0.5392	-5.36500	6
11	15	500	750	120	90	0.3333	1.0000	0.6667	-3.52139	2
12	15	600	800	90	75	0.4375	0.4421	0.4398	-7.13490	13
13	20	300	900	120	75	0.3679	0.3529	0.3604	-8.86430	16
14	20	400	850	90	90	0.372	0.4252	0.3986	-7.98925	15
15	20	500	800	180	25	0.6443	0.3984	0.5214	-5.65658	8
16	20	600	750	150	50	0.4921	0.4413	0.4667	-6.61924	12

3.5 Effects of the Control Factors on GRG

The dominant control factors were identified from the delta statistics in the response table for signal-noise ratio as shown in Table 8. The delta statistics were computed as reported previously. The highest value of delta was assigned the first rank and represents the predominant factor affecting GRG. From the table, processing temperature (PT) is the most influential factor. The second contributing factor is the stirring speed (SS). The third contributing factor is the particle size (PS), followed by the stirring time (ST), and lastly the reinforcement fraction (CSAp).

Table 8: Response for Signal to Noise Ratios of GRG

Level	CSAp (wt %)	SS (rpm)	PT (oC)	ST (Secs)	PS (µm)
1	-5.733	-6.380	-5.997	-7.037	-4.908*
2	-5.358*	-5.943	-5.829	-5.291*	-6.529
3	-5.581	-5.823	-5.097*	-5.856	-6.834
4	-7.283	-5.809*	-7.032	-5.771	-5.685
Delta	1.925	0.571	1.935	1.746	1.926
Rank	3	5	1	4	2
Optimum	CSAp ₂	SS ₄	PT ₃	ST ₂	PS ₁

*Optimum factor levels

3.6 Confirmation Test

For confirmation, the optimal value was compared with experiment run 8 which had the same parameter settings with the optimal combination (CSAp₂SS₄PT₃ST₂PS₁); coconut shell ash particles (CSAp) at 10wt% (level 2), Stirring speed (SS) at 600 rpm (level 4), Processing temperature (PT) at 850°C (level 3), Stirring time (ST) at 120 secs (level 2) and Particle size (PS) at 25 µm (level 1). The results at the optimal and predicted processing parameters of the Aluminium/Coconut shell ash particles composite are shown in Table 9. The percentage improvement in GRG was also evaluated and found to be within the acceptable range (Ibrahim, 2023)

Table 9 shows how the properties of the composite improved as a result of the analysis carried out at the optimal level. It can be inferred from the table that there was an improvement of 36.4% and 30.7% respectively in the GRG of the experimental and predicted over the initial settings. This improvement in the experimental

results over the initial design parameters affirms the validity of the Taguchi method coupled with grey relational analysis for enhancing the properties of the composite developed (Sylajakumari et al., 2018).

Table 9: Confirmatory Results Comparison at the Optimal Level

Initial Design Parameters		Optimal Design Parameters	
		Experiment No. 4	Predicted
Setting Level	KC _{p1} SS ₁ PT ₁ ST ₁ PS ₁	CSA _{p2} SS ₄ PT ₃ ST ₂ PS ₁	CSA _{p2} SS ₄ PT ₃ ST ₂ PS ₁
Grey Relational Grade	0.5015	0.6840	0.6557
Improvement in GRG (%)		36.4	30.7

3.7 Analysis of Variance (ANOVA) of GRG

ANOVA investigation shows the level of significance of each processing parameter. The analysis was also used to develop the predictive mathematical model for the GRG as a function of the stir casting process parameters.

Table 10 shows that stirring speed with a contribution of 46.66% has the highest influence on the GRG; followed by processing temperature with 25.92%, particle size with 15.65%, stirring time with 5.57%, and reinforcement fraction with 5.19%. At 95% confidence level, factors having *p*-value less than 0.05 are considered significant (Sylajakumari et al., 2018). Since the *p*-values of stirring speed and processing temperature are less than 0.05, they are considered significant contributors to the change in GRG of the composite. Conversely, reinforcement fraction, stirring time, and particle size are said to be insignificant terms, because their *p* values are above 0.05. The predictive mathematical model for the GRG is presented in Equation 7.

$$GRG = 0.876 + 0.00043CSAp + 0.000229SS - 0.000607PT + 0.000126ST + 0.000739PS \quad 7$$

Table 10: Analysis of Variance for GRG of Al/CSAp Composite

Source	DF	Seq SS	Contribution	Adj SS	Adj MS	F-Value	P-Value
Regression	5	0.034623		0.034623	0.006925	4.45	0.022
CSAp	1	0.000094	5.19%	0.000094	0.000094	0.06	0.811
SS	1	0.010497	46.66%	0.010497	0.010497	6.74	0.027
PT	1	0.018398	25.92%	0.018398	0.018398	11.82	0.006
ST	1	0.000287	5.57%	0.000287	0.000287	0.18	0.677
PS	1	0.005347	15.65%	0.005347	0.005347	3.44	0.094
Error	10	0.015564	1.01%	0.015564	0.001556		
Total	15	0.050187	100.00%				

The developed regression model for GRG has high coefficient of determination (R^2), R^2_{adj} and R^2_{pred} values of 98.99%, 93.48%, 84.83%, respectively. This indicates the goodness of fit between the GRG and the stir casting process parameters.

4. Conclusion

This study considered the optimization of the fatigue and compressive strength properties of Al7075 alloy as a matrix reinforced with coconut shell ash particles with possible areas of application in buildings, civil transport, and automobile industries. The fatigue strength of the Aluminium/CSAp composite indicated that the processing temperature significantly affects fatigue strength, while the stirring speed has the greatest effect on compressive strength. Confirmatory experiments carried out using the optimal parameters (CSA_{p2}SS₄PT₃ST₂PS₁) in the GRG showed an improvement in the fatigue and compressive strength of the optimized composite over the initial settings.

References

Adebisi, AA. and Ndaliman, MB. 2015. Mathematical modelling of stir casting process parameters for AlSiCp composite using central composite design. Proceedings of the 28th AGM and International conference of the Nigerian Institution for Mechanical Engineers.

- Aigbodion, VS., Asuke, F., Neife, SI., Edokpia, RO. and Omah, AD. 2014. Production of alumino-silicate clay-bonded bagasse ash composite crucible by slip casting, *J. Mater. Environ. Sc.*, 5(5): 1658-1666.
- Alaneme, KK. and Adewuyi, EO. 2013. Mechanical behaviour of Al-Mg-Si matrix composites reinforced with alumina and bamboo leaf ash, *Metall. Mater. Eng.*, 19(3): 177-187.
- Apasi, A. 2014. Development of metal matrix/coconut shell ash particulate composites for automotive application, Dissertation, Ahmadu Bello University, Zaria.
- Apasi, A. Yawas, DS. Abdulkareem, S. and Kolawole, MY. 2016. Improving Mechanical Properties of Aluminium Alloy Through Addition of Coconut Shell-Ash. *Journal of Science and Technology*, 36(3) 34-43.
- ASTM E606-92 (Reapproved 1998). Standard Practice for Strain-Controlled Fatigue Testing. ASTM International, 100 Barr Harbor Drive, West Conshohocken, United States.
- ASTM E09-89a (Reapproved 2000) Standard Test Methods of Compression Testing of Metallic Materials at Room Temperature. ASTM International, 100 Barr Harbor Drive, West Conshohocken, United States.
- Dan-asabe, B. 2018. Thermo-mechanical characterization of banana particulate reinforced PVC composite as piping material. *Journal of King Saud University - Engineering Sciences*, 30(4): 296-304. doi:10.1016/j.jksues.2016.11.001.
- Franklin, OT. Stephen, AT. Johnson, I. 2022. Determination of Mechanical Properties of Coconut Shell Ash Reinforced Aluminum Metal Matrix Composite. *Proceedings of The 35 International Conference of The Nigerian Institution of Mechanical Engineers*. ISBN 988978 = 968 – 746-6
- Gambo, AV. 2017. Abrasive wear behaviour of Al-Cu-Mg/palm kernel shell ash particulate composite. *Leonardo Electronic Journal of Practices and Technologies*, Issue 31: 77-92.
- Ibrahim, TK. 2023. Development of automobile brake disc using aluminium (6061) matrix reinforced with pumice and carbonated coal. Ph.D Progress Report, Ahmadu Bello Zaria.
- Ibrahim, TK., Yawas, DS., Dan-asabe, B. and Adebisi, AA. 2023a. Taguchi optimization and modelling of stir casting process parameters on the percentage elongation of aluminium, pumice and carbonated coal composite. *Scientific Report*, 13, 2915. doi:10.1038/s41598-023-29839-8.
- Ibrahim, TK., Yawas, DS., Dan-asabe, B., and Adebisi, A.A. 2023b. Manufacturing and Optimization of the Effect of Casting Process Parameters on the Compressive Strength of Aluminum/Pumice/Carbonated Coal Hybrid Composites: Taguchi and Regression Analysis Approach. *International Journal of Advance Manufacturing*, 125: 3401–3414. doi:10.1007/s00170-023-10923-2.
- Kabelmetal Nigeria Plc technical brochure 2022. Available online: <https://kabelmetal-nocaco.com>, retrieved 23rd March, 2025.
- Kumar, R. and Kumar, V. 2017. Optimization of process parameter for stir casted AA6063 metal matrix composite on hardness, tensile strength and impact energy. *International Journal of Mechanical Engineering and Technology*, 8(12): 108–117.
- Kundu, J., and Singh, H. 2016. Frictions stir welding of AA5083 aluminium alloy: multi-response optimization using Taguchi-based grey relational analysis. *Advances in Mechanical Engineering*, 8(11): 1-10.
- Madakson, PB., Yawas, DS. and Apasi, A. 2012. Characterization of Coconut Shell Ash for Potential Utilization in Metal Matrix Composites for Automotive Applications. *International Journal of Engineering Science and Technology*, 4 (03): 1190-1198.
- Pulkit, B. 2012. Mechanical behaviour of aluminum based metal matrix composites reinforced with SiC and Alumina, Thesis, Thapar University, Patiala-India.

Raut, V., Gandhi, M., Nagare, N., and Deshmukh, A. 2016. Application of Taguchi grey relational analysis to optimize the process parameters in wire electrical discharge machine. *International Journal of Innovative Science, Engineering & Technology*, 3(7):108-115.

Sivaiah, P. and Chakradhar, D. 2019. Performance improvement of cryogenic turning process during machining of 17-4 PH stainless steel using multi objective optimization technique. *Measurement*, 136:326-336. doi.org/10.1016/j.measurement.2018.12.094

Sylajakumari, P.A., Ramakrishnasamy, R. and Palaniappan, G. 2018. Taguchi grey relational analysis for multi-response optimization of wear in co-continuous composite. *Materials*, 11:1-17. [doi: 10.3390/ma11091743](https://doi.org/10.3390/ma11091743).

Varalakshmi, K., Kumar, K.C., Babu, A.J. 2019. Analysis of Dry Sliding Wear Behaviour of Al 6061- Coconut Shell Ash Metal Matrix Composites using Stir Casting. *Applied Engineering Letters*, 4(2): 55-65. doi.org/10.18485/aeletters.2019.4.2.3

Yekinni, A.A., Durowaju, M.O., Agunsoye, J.O. and Mudashiru, L.O. 2020. Effect of particle size of rice husk ash on Aluminium/Graphene composites. *IOP Conf. Series: Materials Science and Engineering*, 1-19.